Video Article

# Three-dimensional Imaging and Analysis of Mitochondria within Human Intraepidermal Nerve Fibers

Hussein S. Hamid[1], John M. Hayes[2], Eva L. Feldman[2], Stephen I. Lentz[3]

[1]University of Michigan Medical School

[2]Department of Neurology, University of Michigan

[3]Department of Internal Medicine, University of Michigan

Correspondence to: Stephen I. Lentz at lentzs@med.umich.edu

URL: https://www.jove.com/video/53369
DOI: doi:10.3791/53369

Keywords: Neurobiology, Issue 127, mitochondria, intraepidermal nerve fibers, human skin biopsy, three-dimensional imaging and analysis, small fiber neuropathy

Date Published: 9/29/2017

Citation: Hamid, H.S., Hayes, J.M., Feldman, E.L., Lentz, S.I. Three-dimensional Imaging and Analysis of Mitochondria within Human Intraepidermal Nerve Fibers. *J. Vis. Exp.* (127), e53369, doi:10.3791/53369 (2017).

## Abstract

The goal of this protocol is to study mitochondria within intraepidermal nerve fibers. Therefore, 3D imaging and analysis techniques were developed to isolate nerve-specific mitochondria and evaluate disease-induced alterations of mitochondria in the distal tip of sensory nerves. The protocol combines fluorescence immunohistochemistry, confocal microscopy and 3D image analysis techniques to visualize and quantify nerve-specific mitochondria. Detailed parameters are defined throughout the procedures in order to provide a concrete example of how to use these techniques to isolate nerve-specific mitochondria. Antibodies were used to label nerve and mitochondrial signals within tissue sections of skin punch biopsies, which was followed by indirect immunofluorescence to visualize nerves and mitochondria with a green and red fluorescent signal respectively. Z-series images were acquired with confocal microscopy and 3D analysis software was used to process and analyze the signals. It is not necessary to follow the exact parameters described within, but it is important to be consistent with the ones chosen throughout the staining, acquisition and analysis steps. The strength of this protocol is that it is applicable to a wide variety of circumstances where one fluorescent signal is used to isolate other signals that would otherwise be impossible to study alone.

## Video Link

The video component of this article can be found at https://www.jove.com/video/53369/

## Introduction

Mitochondria serve vital cellular functions that include producing cell energy, buffering calcium, and regulating necrotic and apoptotic cell death[1,2,3]. The nervous system has a high metabolic rate compared to the body[4] suggesting that neurons generate a high degree of cellular energy in the form of adenosine triphosphate (ATP) through mitochondrial respiration. A lot of evidence documents that neuronal functions are dependent on ATP[5], especially at the synapses[6]. Therefore, the distribution of mitochondria within neurons is important.

Over the last 10 years a lot of information has shown that the trafficking and docking of neuronal mitochondria is highly regulated. Motor proteins are involved in distributing mitochondria to specific cellular compartments throughout the neuron. Trafficking of mitochondria is particularly important because neurons project axons and dendrites far away from the soma. Kinesin motor proteins primarily direct anterograde (away from the soma) trafficking of mitochondria along microtubules while dynein motor proteins direct retrograde (toward the soma) motility[7,8,9,10]. There are cellular signals such a mitochondrial membrane potential and impulse conduction that influence the presence and direction of mitochondrial trafficking[11,12,13].

In addition to transporting mitochondria, there are specialized proteins to localize mitochondria to specific cellular compartments that have high energy demands, such as nodes of Ranvier and synapses[8,14,17]. In fact, the majority of mitochondria within axons are non-motile[9,13,18]. Specialized proteins like syntaphilin anchor mitochondria to microtubules along axons while other proteins anchor mitochondria to the actin cytoskeleton[19-21]. Growth factors and ions such as calcium have been reported to support the cessation of mitochondria movement to localize them to regions where they are needed[21,22,23].

Taken together, the trafficking and docking of mitochondria are vital for proper function of neurons. In support of this, disruption in mitochondrial trafficking has been associated with several neurological conditions including Alzheimer's disease, amyotrophic lateral sclerosis, Charcot-Marie-Tooth disease, Huntington's disease, hereditary spastic paraparesis, and optic atrophy[15,24,25,26,27]. Recent studies have focused on mitochondrial dysfunction and pathology as a potential mechanism for diabetic neuropathy, the sensory loss associated with diabetes[28,29,30,31,32,33]. The hypothesis is that diabetes alters the distribution of mitochondria within the sensory projections of cutaneous nerve ending. Therefore, a technique was developed to visualize and quantify mitochondria within the intraepidermal nerve fibers (IENFs), the distal tips of dorsal root ganglion sensory afferents. The technique combines fluorescence immunohistochemistry of specific mitochondrial and nerve fiber labels with

 

confocal microscopy z-series acquisition of signals with powerful 3D image analysis software to measure the distribution of nerve-specific mitochondria from human cutaneous punch biopsies to achieve this goal.

## Protocol

Skin punch biopsies were obtained from subjects that were recruited from a large community-based primary care network at the University of Utah Diabetes Center (Salt Lake City, UT). This study was approved by the University of Michigan Institutional Review Board and complied with the tenets of the Declaration of Helsinki. Written informed consent was obtained from each subject prior to testing.

# 1. Fluorescence Immunohistochemistry

1. **Prepare punch biopsies for intraepidermal nerve fiber immunohistochemistry:**
    1. Perform 3 mm skin biopsies by medical staff and place the whole biopsy in 1.5 mL Zamboni's fixative solution (2% paraformaldehyde, 0.3% saturated picric acid in phosphate buffered saline (PBS), pH 7.4) at 4 °C overnight.
    2. Rinse samples with a solution of 30% sucrose in PBS at 4 °C for 16-24 h or until the sample sinks.
    3. Embed samples in optimal cutting temperature compound (OCT) using a cryomold. Place the whole 3 mm biopsy with the epidermis facing down in the mold and fill the mold with approximately 2 mL of OCT. Freeze the mold on crushed dry ice. Store at -80 °C until ready to use.
    4. Cut 50 µm thick cross sections using a cryostat and store in individual wells of a 96-well plate using 180 µL antifreeze storage solution per well (30% ethylene glycol, 30% glycerol in PBS). The following directions are for 8 wells of a 96 well plate. Stain sections from each biopsy site that are 200 - 300 µm away from each other.

DAY 1:

2. **Quench non-specific labeling of the stratum corneum:**
    1. Label 96-well plate as shown in **Figure 1**.
    2. Pipet 150 µL of stock signal enhancer solution to reduce nonspecific binding of secondary antibodies[34,35] into each well. Transfer sections into signal enhancer solution using an inoculating loop.
    NOTE: Take care while working with the tissue to avoid damaging or tearing the tissue sections. Keep in signal enhancer solution for 30 minutes at room temperature on a flat rocker.
    3. Prepare rinse wells in rows 2 and 3 of the 96-well plate by adding 150 µL of 1x phosphate buffered saline (PBS) into each well.
    4. Carefully transfer sections into row 2 and rinse in 1x PBS for 10 min at room temperature.
    5. Rinse a second time in 1x PBS for 10 min at room temperature (row 3).

3. **Prepare 5% bovine serum albumin (BSA) blocking solution:**
    1. Prepare 5% blocking solution that contains 5% BSA and 0.3% Triton X 100 (TX-100) in 0.1 M PBS (see **Table 1**) while sections are incubating in signal enhancer solution. BSA does not go into solution easily. Vortex solution until BSA completely dissolves.
    2. Prepare blocking wells in row 4 of the 96-well plate by adding 150 µL of 5% BSA blocking solution into each well.
    3. Transfer sections into individual wells of 5% BSA blocking solution and incubate sections in 5% BSA blocking solution for 1 - 2 h at room temperature on a flat rocker.

4. **Prepare 1% BSA rinsing solution and dilution of primary antibodies:**
    1. Prepare 1% rinsing solution that contains 1% BSA and 0.3% TX-100 in 0.1 M PBS (see **Table 2**) while sections are incubating in 5% BSA blocking solution. BSA does not go into solution easily. Vortex solution until BSA completely dissolves.
    2. Dilute primary antibodies in 1% BSA rinsing solution while sections are incubating in 5% BSA blocking solution.
        1. Make 1,500 µL of primary antibody solution and add to each well in row 5.
        2. Dilute the primary antibodies: Use the nerve-specific label, rabbit polyclonal anti-protein gene product 9.5 (PGP9.5) at 1:1,000. Use the mitochondria-specific label, mouse monoclonal anti-pyruvate dehydrogenase E2/E3bp antibody (PDH) at 1:100 in 1% BSA rinsing solution.

5. **Prepare primary antibody:**
    1. Pipet 150 µL of primary antibody into each well in row 5 of the 96-well plate.
    2. Using the loop tool, transfer sections from the blocking solution (row 4) into the row 5 containing the primary antibody.
    3. Wrap the plate tightly with parafilm to keep it from drying out.
    4. Place samples on flat rocker at room temperature for 1 h, and then incubate samples at 4 ºC on a flat rocker overnight.

DAY 2:

6. **Rinse samples:**
    1. Prepare rinse wells in rows 6, 7 and 8 of the 96-well plate by adding 150 µL of 1% BSA rinsing solution into each well.
    2. Transfer sections into first 1% BSA rinsing solution (row 6) and incubate for 1 h at room temperature. Repeat rinses twice more by incubating sections in 1% BSA rinsing solution in rows 7 and 8 for 1 h each at room temperature.

7. **Dilute secondary antibodies in 1% BSA rinsing solution:**
    1. Make 1,500 µL of secondary antibody solution while sections are incubating in the last rinse of 1% BSA rinsing solution (row 8).

2. Dilute secondary antibodies: for PGP9.5 (green-fluorescent conjugated goat anti-rabbit antibody, 1:1000), for PDH (red-fluorescent conjugated goat anti-mouse, 1:1,000) in 1% BSA rinsing solution.

8. **Prepare secondary antibody:**
    1. Pipet 150 µL of secondary antibody into row 9 of the 96-well plate.
    2. Gently transfer the sections from 1% BSA rinsing solution (row 8) into secondary antibody wells (row 9).
    3. Using parafilm, wrap the plate tightly to keep it from drying out. Cover with aluminum foil. Place samples on flat rocker at room temperature for 1 h, and then incubate samples at 4 ˚C on a flat rocker overnight.

DAY 3:

9. **Prepare clean 1x PBS by filtering through a 0.22 µm filter:**
    1. Pipet 150 µL of filtered 1x PBS into row 10, 11, and 12.
    2. Transfer samples to row 10 and rinse in 1x PBS for 1 h at room temperature. Cover the 96-well plate with aluminum foil and place on a flat rocker during rinse. Repeat filtered 1x PBS rinse two more times for 1 h each at room temperature in rows 11 and 12.

10. **Prepare microscope slides for mounting tissue sections:**
    1. Place 50 µL of filtered 1x PBS on a slide.
    2. Transfer section from 1x PBS (row 12) into the 50 µL drop. Carefully position the section in the drop of PBS by unfolding the tissue and gently flattening it onto the glass slide. Remove excess PBS with a glass pipette to avoid diluting the mounting reagent. Do not touch sections with the glass bulb.
    3. Pipet 1 - 2 drops of mounting reagent containing DAPI directly on top of the section on the microscope slide using care to not disturb the orientation of the section. Gently place a 50 mm x 24 mm #1.5 microscope glass coverslip over the section.
    4. Clear any air bubbles that formed while placing the coverslip and wipe excess liquid off the edges of the coverslip. Prepare a new slide and repeat the mounting process for each section.
    5. Cure/dry the mounting media by placing the slides in the dark overnight at room temperature. Transfer the slides to 4 °C for short-term (1 - 2 weeks) or -20 °C for long-term storage (greater than 2 weeks).
    NOTE: Negative controls omitted primary antibodies for PGP9.5 or PDH in step 1.4.2.2 and displayed no distinguishable labeling of nerves or mitochondria in the epidermis. Positive controls were performed for the PDH antibody to prove it labels all mitochondria (data not shown). Positive controls were performed on cultured primary mouse dorsal root ganglion neurons that were transduced with a baculovirus to label mitochondria with a Green Fluorescent Protein (GFP) signal and then fixed and stained with the PDH antibody and red fluorescent secondary antibody. All mitochondria that were expressing GFP were co-labeled with the red label for PDH immunohistochemistry (data not shown).

## 2. Confocal Imaging

1. **Perform confocal imaging:**
    1. Collect images using a laser scanning confocal microscope with a 40X oil-immersion (1.25 numerical aperture (N.A.)) objective on an inverted microscope.
        1. At each focal plane sequentially acquire fluorescent signals:
        Nuclei: excitation λ = 405 nm, spectral emission filter λ = 420 - 480 nm
        Nerve fibers: excitation λ= 488 nm, spectral emission filter λ = 505 - 560 nm
        Mitochondria: excitation λ = 543 nm, spectral emission filter λ= 606 - 670 nm

    2. Enter the following scan parameters into the microscope software: scan rate of 600 Hz with 2 frame averaging and zoom of 2.2; 12-bit intensity resolution (4096 gray levels).
        1. Set the microscope software for optimized lateral resolution (scan resolution = 1,024 x 1,024) and axial resolution/optical sectioning (confocal aperture = 1 airy unit (AU) with z-step size of 210 nm).
        NOTE: The resulting XYZ resolution is 172.2 nm x 172.2 nm x 210 nm with an image size of 176.1 µm x 176.1 µm x 30-50 µm.

    3. Activate a live scan for the nerve signal (green-fluorescence) and adjust the z-focus control to find and set the upper and lower focal planes in the microscope software that encompass the nerve signal within the tissue section. The total z-range is typically 30-50 µm for a 50 µm tissue section.
    4. Rotate the scan field with the microscope software during a live scan so that the epidermis is horizontally or vertically positioned in the image.
    5. Scan each signal separately and adjust the detector (photomultiplier tube, PMT) voltage and offset to minimize/remove any over and under saturated pixels.
    NOTE: Scan times with the above parameters take approximately 20 - 40 min depending on the number of z slices.

## 3. 3D Visualization and Analysis of Mitochondria within Human Intraepidermal Nerve Fibers

1. **Isolate the 3D epidermis:**
    1. Duplicate the original image and use the maximum intensity projection (extended focus view) of the image to identify and isolate the epidermis.
    2. Use a region of interest tool to trace along the upper and lower edges of the epidermis to remove unwanted areas such as the stratum corneum and dermis that are absent of intraepidermal nerve fibers. Crop to this selection.

2. **Use deconvolution on the nerve and mitochondrial fluorescent signals:**
NOTE: Deconvolution helps to restore the integrity of the fluorescent signals. The restoration used in this protocol is called blind deconvolution because it uses the fluorescent signals in the images to determine how much the signals spread from their original source (point spread function). The process improves signal resolution by reassigning the signal spread back to its origin location.
    1. Calculate a point spread function (PSF) for the green fluorescent nerve signal (green-fluorescence) with the following parameters:
        1. Set calculated PSF to confocal. Set medium refractive index to 1.515 and numerical aperture to 1.25. Set detector pinhole to 1 Airy unit (A.U.). Set laser excitation wavelength to 488 nm and emission wavelength to 515 nm.

    2. Calculate a PSF for the red fluorescent mitochondrial signal (red-fluorescence) with the following parameters:
        1. Set calculated PSF to confocal. Set medium refractive index to 1.515 and numerical aperture to 1.25. Set detector pinhole to 1 AU. Set laser excitation wavelength to 543 nm and emission wavelength to 617 nm.

    3. Optimize the nerve and mitochondria fluorescent signals by deconvolution using the corresponding PSFs listed above and iterative restoration feature set at 100% confidence and an iteration limit of 10 cycles.

3. **Create nerve-specific surfaces:**
    1. Use the "create surface" tool to make a solid surface of the nerves from the deconvolved green- fluorescent secondary labeling of the PGP9.5 identified nerves.
    2. Uncheck the "smooth" feature and use the absolute intensity feature to set the threshold for the nerve signal since it is significantly brighter than background fluorescence.
    3. Use the absolute intensity feature to set the threshold for the nerve signal since it is significantly brighter than background fluorescence. Set threshold value low enough to accurately identify the nerves.
    4. Filter out small, non-nerve surfaces based on size.
    NOTE: If necessary, manually edit out additional non-nerve surfaces within the "Edit" tab by holding the CONTROL key to highlight multiple objects and then deleting them with the Delete key.

4. **Isolate nerve-specific fluorescent mitochondrial signal:**
    1. Select the Edit tab of the nerve surface to view the "Mask Properties" feature. The nerve surface created in steps 3.3 is used to isolate mitochondria within those nerves away from mitochondrial signals associated with the keratinocytes.
    2. As the "Mask All' button opens a "Mask Channel" window, choose the deconvolved red-fluorescent signal from the pull down menu under "Channel Selection" for the mitochondrial signal.
    3. Click in the box to put a check mark in the "duplicate channel before applying mask" option.
    4. Click on the radio button in front of the "Constant inside/outside" option of the Mask Settings and click in the box to put a check mark in the "Set voxel outside surface to" option and type in 0.00 for the value. Click OK button to create the new channel that represents mitochondrial signals within the nerve surface.

5. **Create mitochondria-specific surfaces:**
    1. Use the "create surface" tool to make a solid surface of the mitochondria from the newly created fluorescent channel of the nerve-specific mitochondrial signals from steps 3.4.
    2. Uncheck the "smooth" feature and select the "background subtraction" feature to set the threshold. This feature uses local contrast around the mitochondrial signal to identify mitochondria from background.
    3. Set threshold value low enough to accurately identify mitochondria. In this example the lower threshold was set at 2,000 for a 16-bit (65,536) scale.
    4. Filter mitochondrial surfaces based on size. In this example the voxel limit was set to 1.0 voxels, which is the lowest limit possible. If necessary, manually edit out non-mitochondria surfaces within the "Edit" tab by holding the CONTROL key to select multiple objects and then deleting them with the Delete key.
    NOTE: Occasionally, the software will create surfaces that are not associated with a distinguishable fluorescent mitochondrial signal. In these cases, it is possible to remove them with the "Edit" tab.

6. **Export and calculate morphometric values for analysis:**
    1. Export values for nerve and mitochondrial surfaces from the "Statistics" tab for further analysis with electronic spreadsheet software.
    2. Export the volume values for both the nerve and mitochondrial surfaces.
    3. Count the number of individual nerve fibers present in each image and record the value in the electronic spreadsheet.
    4. For each image, calculate the following potential values for analysis in the electronic spreadsheet:
        1. Sum the volumes for all nerve surfaces.
        2. Filter out nerve-specific mitochondrial surfaces below a volume of less than 0.02 $\mu m^3$ and bin the surfaces by size. For example, use bins such as 0.02 - 0.04, 0.04 - 0.08, 0.08 - 0.16, 0.16 - 0.32, 0.32 - 0.64, 0.64 - 1.28, 1.28 - 2.56, greater than 2.56 $\mu m^3$.
        NOTE: The lower limit of mitochondrial volume was set to 0.02 $\mu m^3$ based on previously published volumes of mitonchodria[36,37,38].
        3. Count the number of nerve-specific mitochondrial surfaces within each bin and the total number of surfaces over the bins (0.02 - greater than 2.56 $\mu m^3$).
        4. Calculate the proportion of nerve-specific mitochondrial surfaces in each bin. Use the count per bin divided by the total number of mitochondria surfaces.
        5. Sum the volumes for all nerve-specific mitochondrial surfaces.
        6. Calculate the proportion of nerve with mitochondrial signal by dividing the total nerve surface volume by the sum of all mitochondrial surface volumes.
        7. Calculate the number of mitochondria per nerve volume by dividing the total nerve surface volume by the count of all mitochondrial surfaces.

## Representative Results

**Visualization and quantification of mitochondria within human IENFs**

Fluorescence immunohistochemistry allows for the simultaneous labeling of multiple signals within human skin biopsies to visualize nerves, mitochondria, and nuclei. A 96-well plate is a convenient way to organize the steps in the immunohistochemistry procedure. **Figure 1** shows that this configuration accounts for up to 8 sections to be processed through the 12 stages of solutions. The free-floating method combined with gentle agitation with a flat rocker ensures that the antibodies have sufficient access to penetrate the sections from both sides. The protocol takes 3 days to complete, which is largely due to overnight incubations in primary and secondary antibodies at 4 °C, which consistently label nerves and mitochondria.

The remainder of the procedure incorporates imaging, processing and analysis of the fluorescent signals. Confocal microscopy takes advantage of the fluorescent signals to optically section discrete signals from the focal plane by eliminating out-of-focus signals. Acquisition of z-series through the tissue section provides a 3D representation of the fluorescent signals for nerves, mitochondria, and nuclei. The parameters are optimized to image 172 µm along the length of the epidermis that would include an average of 5 nerves. **Figure 2** illustrates a typical 3D image of the three fluorescent signals that are collected from the epidermis. The PGP9.5 staining (**Figure 2B**) provides a rich signal of the epidermal and dermal nerves that is of a higher intensity than the background auto-fluorescence of the tissue. The nuclear stain (**Figure 2C**) helps to identify boundaries of the epidermis where the intraepidermal nerve fibers innervate. It is common for the outer layer of the epidermis to have a diffuse signal that might be due to residual DNA in the corneocytes that make up the stratum corneum. The mitochondria are clearly labeled by the PDH staining (**Figure 2D**) where the majority of the signal is associated with cells in the epidermis that are primarily keratinocytes.

The acquisition parameters described in this protocol use a 40X oil immersion objective with a 1.25 numerical aperture and a zoom factor of 2.2. This results in a XYZ image size of 176.1 µm x 176.1 µm x 30 - 50 µm. These settings capture enough of the epidermis to include an average of 4-6 nerve fibers per image (**Figure 3A**). Sampling at higher resolution would reduce the number of nerves in each image. **Figure 3B** shows a zoom factor of 3.3, which reduces the XY area to 114.8 µm x 114.8 µm, resulting in fewer nerves per image. The ideal sampling density as defined by Nyquist (http://www.svi.nl/NyquistCalculator) for a 40x oil immersion objective with a 1.25 numerical aperture suggests a XYZ scan resolution of 54 nm x 54 nm x 205 nm. This would require a zoom factor of 6.6 fold at 1,024 x 1,024 resolution and reduce the XY view to 57.4 µm x 57.4 µm and only capture an average of 1 - 2 nerve per image (**Figure 3C**).

The next phase is to perform image processing to remove unwanted regions of the image and to enhance the signals. In this protocol the dermis and stratum corneum are removed in order to focus the analysis on the region of the epidermis where the IENFs innervate. Three-dimensional software makes it possible to isolate, enhance and analyze the fluorescent signals. Tools within the software are needed to isolate the epidermal nerve and mitochondria by cropping out regions above and below the epidermis (**Figure 4A-C**). This process is simplified by collapsing the signals into an extended view and then tracing a freehand region around the epidermis. The cropped image is further processed by image restoration algorithms. Deconvolution is used to optimize the resolution of the nerves and mitochondrial signals (**Figure 4D**).

The final phase is to detect and extract morphometric features from the signals. An important aspect of this protocol is to measure features of nerve-specific mitochondria. Image analysis software has features that use surfaces created for one signal (in this case the nerve surface) as a masking tool to isolate another fluorescent signal (in this case mitochondria) within that surface. The first step in the analysis of nerve-specific mitochondria is to create 3D surfaces around nerves (**Figure 5A-B**). The nerve surfaces are then used to crop the nerve-specific fluorescent mitochondrial signals (**Figure 5C**, 5**D**, **5E**, **5G**). Finally, 3D surfaces are created around the nerve-specific mitochondrial signals to obtain volumetric measurements (**Figure 5F**, 5**H**). **Table 3** shows the morphometric measurements that are exported from the image analysis software and summary data. The main values to export are the volume values for the nerve and nerve-specific mitochondrial signals. The volume data from the mitochondria are binned to generate mitochondria size frequency data, which is then used to create size frequency histograms (**Figure 6**). The volume data are also used to make summary measures for number of mitochondria per IENF volume and percentage of mitochondrial volume within IENF volumes.

The data presented in Table 3 and **Figure 6** demonstrate that this technique provides a means to quantify mitochondria within human IENFs from skin biopsies. The nerves from this sample have mitochondria distributed throughout and the majority of mitochondria are between 0.02 - 0.32 $\mu m^3$. These sizes are in a range associated with normal mitochondria[36,37,38,39]. Smaller mitochondria have been shown to be more motile than larger mitochondria[39] suggesting that the mitochondria in these nerves might be more motile. Indeed, studies have implicated that larger, swollen mitochondria do not transport as well as smaller mitochondria and may lead to axonal degeneration[39,40,41]. Therefore, characterization of nerve-specific mitochondria is a valuable technique that would be applicable to studies of neurodegenerative diseases where changes in mitochondrial morphology and transport have been associated with axonal degeneration[15,25,26,27,42,43].

| 5% BSA Blocking Solution | |
|---|---|
| Components of 5% BSA Blocking Solution | Amount Needed |
| Bovine Serum Albumin (BSA) [Final Concentration: 5%] | 0.625 g |
| 1.0% Triton X-100 (TX-100) [Final Concentration: 0.3%] | 3.75 mL |
| 1x PBS | ~8.125 mL |
| **TOTAL** (use 1X PBS to bring total volume to 12.5 mL) | 12.5 mL |

**Table 1: 5% BSA Blocking Solution.** The 5% BSA blocking solution is used in early steps of the immunohistochemistry protocol to block non-specific binding of the antibodies.

| 1% BSA Rinsing Solution | |
|---|---|
| Components of 1% BSA Rinsing Solution | Amount Needed |
| Bovine Serum Albumin (BSA) [Final Concentration: 1%] | 0.125 g |
| 1.0% TX-100 [Final Concentration: 0.3%] | 3.75 mL |
| 1x PBS | ~8.125 mL |
| **TOTAL** (use 1X PBS to bring total volume to 12.5 mL) | 12.5 mL |

**Table 2: 1% BSA Rinsing Solution.** The 1% BSA rinsing solution is used in the immunohistochemistry protocol to block non-specific binding of the antibodies and used for diluting primary and secondary antibodies.

| Morphometric Measurements for IENFs and Nerve-Specific Mitochondria | | | | | | | | |
|---|---|---|---|---|---|---|---|---|
| Exported and Summary Data from Image Analysis Software | | | | | | | | |
| Mt Size Frequency Bins | Number of Mt in Size Frequency Bin | Percentage of Mt in Bin | Total Number of Mt | Mt Volume ($\mu m^3$) | IENF Volume ($\mu m^3$) | Number of Mt per IENF Volume (number/100 $\mu m^3$) | Percentage of Mt Volume in IENF Volume | Number of IENFs |
| between .02-.04 $\mu m^3$ | 20 | 24.4% | 82 | 13.41 | 518.88 | 15.8 | 2.58% | 4 |
| between .04-.08 $\mu m^3$ | 28 | 34.1% | | | | | | |
| between .08-.16 $\mu m^3$ | 14 | 17.1% | | | | | | |
| between .16-.32 $\mu m^3$ | 12 | 14.6% | | | | | | |
| between .32-.64 $\mu m^3$ | 4 | 4.9% | | | | | | |
| between .64-1.28 $\mu m^3$ | 3 | 3.7% | | | | | | |
| between 1.28-2.56 $\mu m^3$ | 1 | 1.2% | | | | | | |
| between 2.56+ $\mu m^3$ | 0 | 0.0% | | | | | | |

**Table 3: Morphometric Measurements for IENFs and Nerve-Specific Mitochondria.** The table represents morphometric values that are measured and exported from image analysis software and summary data. Abbreviations: IENF, intraepidermal nerve fibers; Mt, mitochondria.

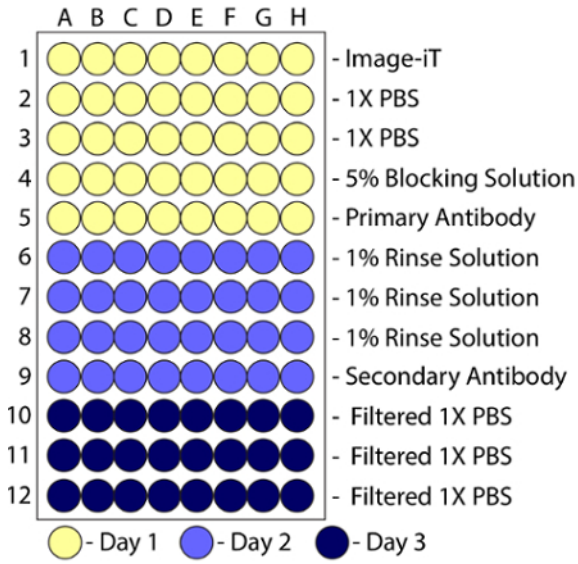


**Figure 1: Schematic Diagram Representing the Setup for a 96-well Plate for Skin Biopsy Immunohistochemistry**. Rows in the plate represent steps in the protocol for block, wash and incubation solutions and columns represent individual tissue sections (from 1 to 8 sections per plate). Please click here to view a larger version of this figure.

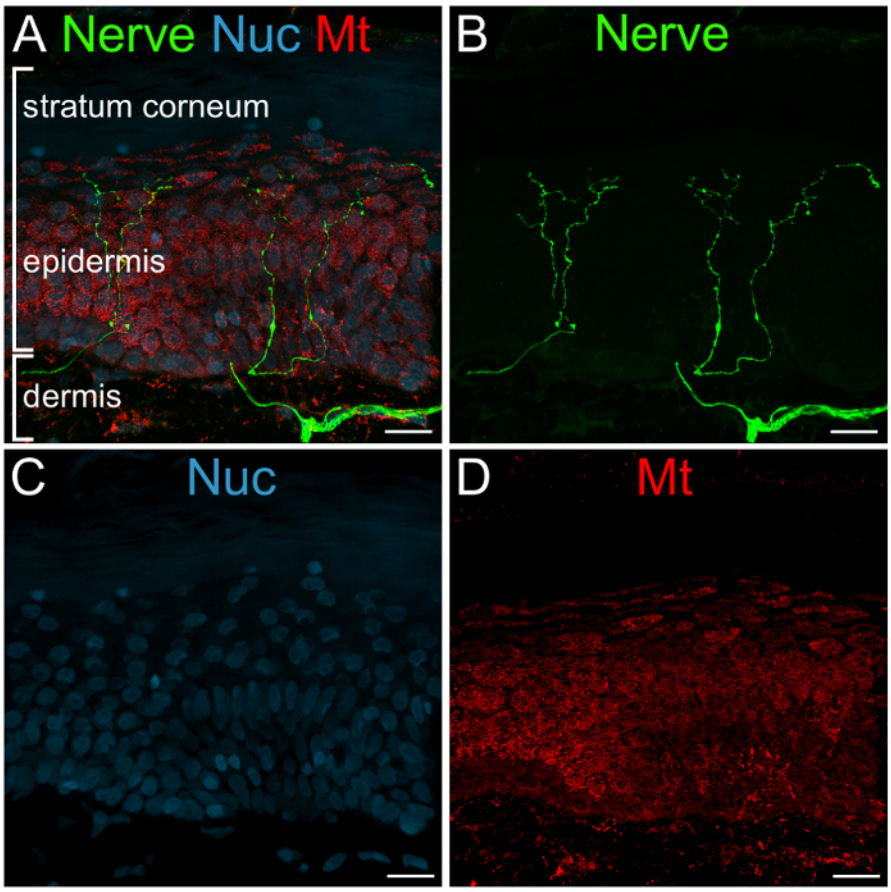


**Figure 2: Representative 3D Confocal Microscopy Image of a Tissue Section from a Human Epidermal Biopsy Processed for Fluorescence Immunohistochemistry.** Unprocessed 3D projection image illustrates the **(A)** merged fluorescent signals and individual signals for **(B)** nerves (Nerve, green), **(C)** nuclei (Nuc, blue) and **(D)** mitochondria (Mt, red) in the epidermis and dermis. Note the lack of signals in the stratum corneum layer of the epidermis. Scale bars = 20 µm. Please click here to view a larger version of this figure.

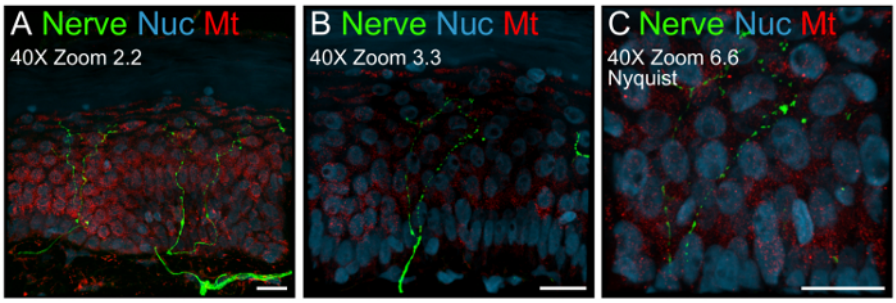


**Figure 3: Improved Image Resolution Results in Fewer Nerves for Subsequent Analysis.** All images are captured with a 40X oil objective with a 1.25 numerical aperture and the 3D projections illustrate fluorescent signals for nerves (green), mitochondria (Mt, red) and nuclei (Nuc, blue). An image taken at a zoom factor of 2.2 **(A)** contains several nerves within the view. Increasing the zoom factor to 3.3 **(B)** or 6.6 **(C)**, the ideal Nyquist sampling, significantly reduces the number of nerves within each image. Scale bars = 20 µm. Please click here to view a larger version of this figure.

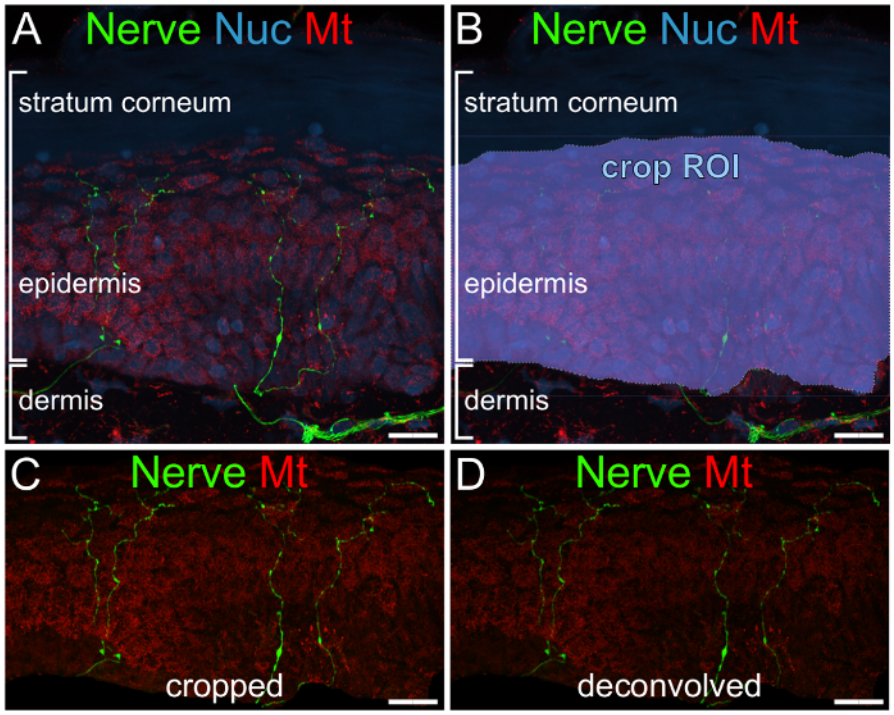


**Figure 4: Image Processing.** Representative extended focus (maximum intensity projection) view of an image from confocal microscopy of a tissue section from a human epidermal biopsy. Unprocessed projection image illustrates **(A)** the merged fluorescent signals for nerves (green), nuclei (Nuc, blue) and mitochondria (Mt, red). The dermis and stratum corneum are **(B)** cropped out with a region of interest (ROI) freehand selection tool (blue highlighted area, crop ROI) isolating only signals in the epidermis. The **(C)** cropped epidermis is then processed for **(D)** deconvolution with calculated point spread functions to improve the resolution of the nerves (green) and mitochondrial (Mt, red) signals. Scale bars = 20 µm. Please click here to view a larger version of this figure.

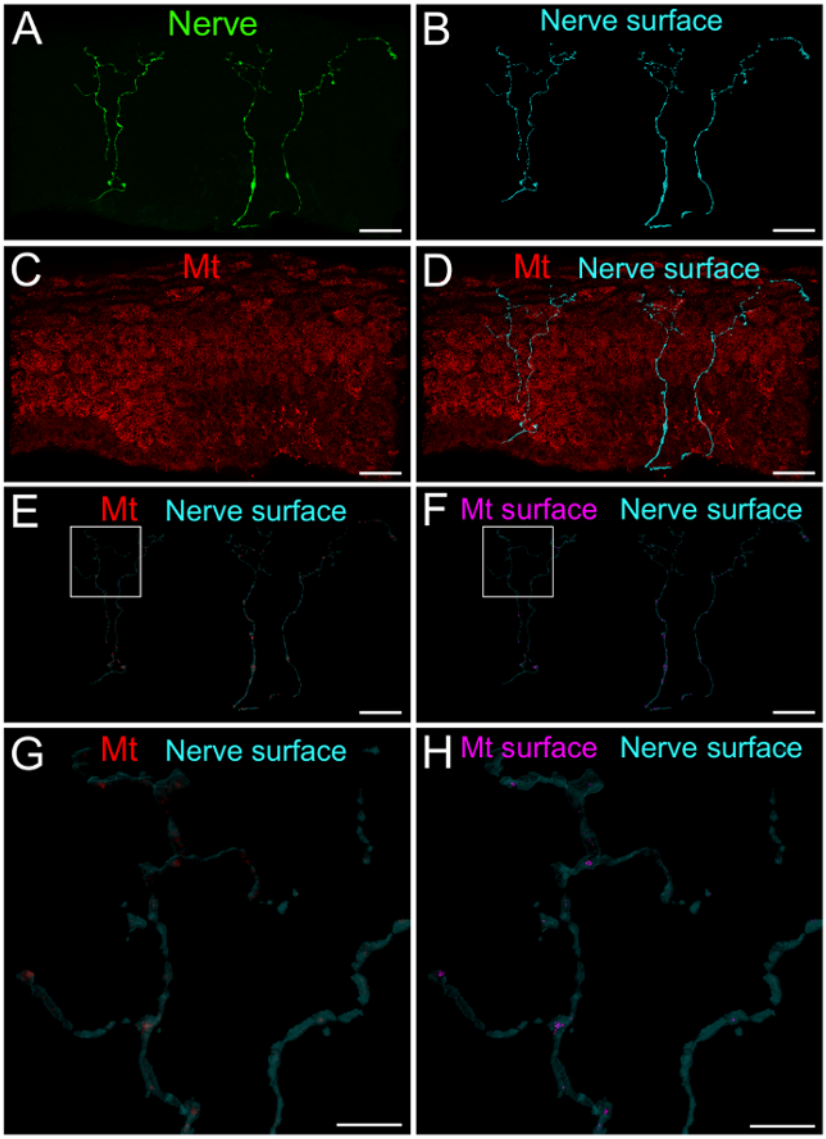


**Figure 5: Image Analysis.** Representative 3D confocal microscopy image illustrates (A) the nerve-specific green fluorescent signal. **(B)** A 3D surface (cyan) is created for the nerve signal. The nerve-specific mitochondrial signal is isolated from the rest of the **(C)** epidermal mitochondrial signals (Mt, red) by **(D)** using the nerve surface as a masking tool. The resulting **(E, G)** nerve-specific mitochondrial red fluorescent signal is used to create (**F, H)** surfaces (Mt surface, magenta) around the mitochondria within the nerve surface (cyan). G and H are magnified views of the white boxes in E and F. Scale bars = 20 µm (A-F), 5 µm (G-H). Please click here to view a larger version of this figure.

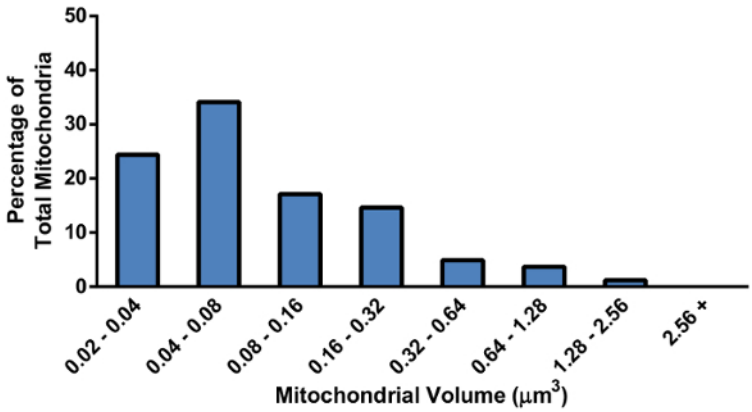


**Figure 6: Mitochondrial Size Frequency Histogram.** Mitochondrialsurface data are presented as a size frequency histogram to visualize the percentage of mitochondria that are present in each of the various bins according to their volume ($\mu m^3$). Please click here to view a larger version of this figure.

## Discussion

This protocol is designed to isolate, quantify and analyze the size and distribution of nerve-specific mitochondria within IENFs in 3D from human skin biopsies. There are several critical steps in the protocol. The free-floating fluorescence immunohistochemistry is designed to stain and analyze multiple signals in each sample, providing a more versatile methodology for explorative research[44,45]. This procedure allows for penetration of the antibodies into the tissue in order to maximize the acquisition of images throughout the 50 µm section, which is necessary for acquiring confocal microscopy images and 3D analysis. Another critical step is the image acquisition parameters that are balanced between capturing enough nerves per image while maintaining resolution for measuring mitochondria. The tissue sections used in this and standard skin biopsy protocols are approximately 3 mm long[45,46,47,48]. The acquisition parameters described in this protocol capture enough of the epidermis to include an average of 4-6 nerve fibers per image. Sampling at higher resolution would significantly reduce the number of nerves in each image, especially at Nyquist sampling. A third critical step is to use deconvolution algorithms to improve the resolution and contrast of the signals, especially for mitochondria. Deconvolution of the images helped to compensate for not sampling at higher resolution. The last critical step is to use image analysis software to isolate nerve-specific mitochondria from the mitochondria associated with cells in the epidermis. This is accomplished by using the nerve surface as a masking tool to crop out mitochondrial signal that localize within the nerve.

There are some potential modifications of this technique to consider. One possible modification would be to shorten the duration of the fluorescence immunohistochemistry. The overnight incubations in the primary and secondary antibody solutions at 4 °C could be shortened to 3-4 hours at room temperature. However, shorter incubations at room temperature often increase background fluorescence, so caution should be taken to avoid poor signal to noise. Another possible modification would be to adjust the image acquisition parameters. As mentioned above, the image acquisition described here were biased toward capturing a reasonable number of nerves per image over high image resolution. It is possible to use a higher magnification objective, such as a 63x oil immersion objective with a 1.3 numerical aperture. If all parameters remained the same and a 63X objective was used, the XY image field would be reduced to 112 µm x 112 µm and therefore reduce the average number of nerves per image. The main point is to use consistent parameters throughout the acquisition and subsequent analysis.

The main limitation of this technique is that it is time consuming. The immunohistochemistry takes 3 days to process tissue, image acquisition takes about 30 - 50 min per image depending how many optical z-steps are taken, and image processing/analysis takes approximately 20 min. This is a significant time commitment but yields important morphometric measurements in the end. Another limitation of this technique is the limited area of epidermis sampled per image. However, this will undoubtedly improve as advancements are made in image acquisition rates with improved resolution combined with faster computer processors and analysis software.

The significance of this protocol over other methods is in the power of combining fluorescence immunohistochemistry with confocal microscopy and 3D image analysis. Traditionally, intraepidermal nerve fiber analysis is done with chromogen based immunohistochemistry and bright-field microscopy, especially for clinical diagnosis of neuropathy[45,47,49]. The use of fluorescence immunohistochemistry makes it possible to stain and analyze multiple signals in each sample, providing a more versatile methodology for explorative research[44,45]. This technique provides a strategy to isolate a particular signal of interest, in this case nerve-specific mitochondria, from a complex signal, mitochondria associated with epidermal cells.

The power of this technique is its usefulness in future applications. The ability to isolate and measure nerve-specific mitochondria makes it possible to evaluate disease-induced alteration in the size and distribution of mitochondria. Multiple neurological complications have implicated mitochondrial dysfunction as a potential mechanism of the disease. In particular, a modified version of this technique has been used to demonstrate that patients with diabetes and diabetic peripheral neuropathy have measureable changes in the size and distribution of nerve-specific mitochondria compared to age-matched controls[50]. This technique would be useful for evaluating the effectiveness of therapies designed to improve or cure sensory neuropathies. Finally, the versatility of the technique makes it applicable to a wide range of analyses that use one fluorescent signal to isolate a subset of data from other fluorescent signals.

## Disclosures

No conflicts of interest to declare.

## Acknowledgements

This work was supported by National Institutes of Health Grants K08 NS061039-01A2, The Program for Neurology Research & Discovery, and The A. Alfred Taubman Medical Research Institute at the University of Michigan. This work used the Morphology and Image Analysis Core of the Michigan Diabetes Research Center, funded by National Institutes of Health Grant 5P90 DK-20572 from the National Institute of Diabetes and Digestive and Kidney Diseases. The authors would like to thank J. Robinson Singleton and A. Gordon Smith (University of Utah) for their generous donation of human skin samples.

## References

1. Nicholls, D. G., & Budd, S. L. Mitochondria and neuronal survival. *Physiol Rev.* **80** (1), 315-360 (2000).
2. Chan, D. C. Mitochondrial fusion and fission in mammals. *Ann Rev Cell Dev Biol.* **22**, 79-99 (2006).
3. Ni, H. M., Williams, J. A., & Ding, W. X. Mitochondrial dynamics and mitochondrial quality control. *Redox Biol.* **4** (C), 6-13 (2015).
4. Mink, J. W., Blumenschine, R. J., & Adams, D. B. Ratio of central nervous system to body metabolism in vertebrates: its constancy and functional basis. *Am J Physiol.* **241** (3), R203-212 (1981).
5. Ames, A., 3rd. CNS energy metabolism as related to function. *Brain Res Brain Res Rev.* **34** (1-2), 42-68 (2000).
6. Harris, J. J., Jolivet, R., & Attwell, D. Synaptic energy use and supply. *Neuron.* **75** (5), 762-777 (2012).
7. Hollenbeck, P. J. The pattern and mechanism of mitochondrial transport in axons. *Front Biosci.* **1**, d91-102 (1996).
8. Cai, Q., & Sheng, Z. H. Mitochondrial transport and docking in axons. *Exp Neurol.* **218** (2), 257-267 (2009).
9. Schwarz, T. L. Mitochondrial trafficking in neurons. *Cold Spring Harb Perspect Biol.* **5** (6) (2013).
10. Saxton, W. M., & Hollenbeck, P. J. The axonal transport of mitochondria. *J Cell Sci.* **125** (Pt 9), 2095-2104 (2012).
11. Sajic, M. *et al.* Impulse conduction increases mitochondrial transport in adult mammalian peripheral nerves in vivo. *PLoS Biol.* **11** (12), e1001754 (2013).
12. Ohno, N. *et al.* Myelination and axonal electrical activity modulate the distribution and motility of mitochondria at CNS nodes of ranvier. . *J Neurosci.* **31** (20), 7249-7258 (2011).
13. Miller, K. E., & Sheetz, M. P. Axonal mitochondrial transport and potential are correlated. *J Cell Sci.* **117**, 2791-2804 (2004).
14. Macaskill, A. F. *et al.* Miro1 is a calcium sensor for glutamate receptor-dependent localization of mitochondria at synapses. *Neuron.* **61** (4), 541-555 (2009).
15. Sheng, Z. H., & Cai, Q. Mitochondrial transport in neurons: impact on synaptic homeostasis and neurodegeneration. *Nat Rev Neurosci.* **13** (2), 77-93 (2012).
16. Berthold, C. H., Fabricius, C., Rydmark, M., & Andersen, B. Axoplasmic organelles at nodes of Ranvier. I. Occurrence and distribution in large myelinated spinal root axons of the adult cat. *J Neurocytol.* **22** (11), 925-940 (1993).
17. Fabricius, C., Berthold, C. H., & Rydmark, M. Axoplasmic organelles at nodes of Ranvier. II. Occurrence and distribution in large myelinated spinal cord axons of the adult cat. *J Neurocytol.* **22** (11), 941-954 (1993).
18. Hollenbeck, P. J., & Saxton, W. M. The axonal transport of mitochondria. *J Cell Sci.* **118** (Pt 23), 5411-5419 (2005).
19. Ohno, N. *et al.* Mitochondrial immobilization mediated by syntaphilin facilitates survival of demyelinated axons. *Proc Natl Acad Sci U S A.* **111** (27), 9953-9958 (2014).
20. Kang, J. S. *et al.* Docking of axonal mitochondria by syntaphilin controls their mobility and affects short-term facilitation. *Cell.* **132** (1), 137-148 (2008).
21. Chada, S. R., & Hollenbeck, P. J. Nerve growth factor signaling regulates motility and docking of axonal mitochondria. *Curr Biol.* **14**, 1272-1276 (2004).
22. Yi, M., Weaver, D., & Hajnoczky, G. Control of mitochondrial motility and distribution by the calcium signal: a homeostatic circuit. *J Cell Biol.* **167** (4), 661-672 (2004).
23. Saotome, M. *et al.* Bidirectional Ca2+-dependent control of mitochondrial dynamics by the Miro GTPase. *Proc Natl Acad Sci U S A.* **105** (52), 20728-20733 (2008).
24. Schon, E. A., & Przedborski, S. Mitochondria: the next (neurode)generation. *Neuron.* **70** (6), 1033-1053 (2011).
25. Petrozzi, L., Ricci, G., Giglioli, N. J., Siciliano, G., & Mancuso, M. Mitochondria and neurodegeneration. *Biosci Rep.* **27** (1-3), 87-104 (2007).
26. Maresca, A., la Morgia, C., Caporali, L., Valentino, M. L., & Carelli, V. The optic nerve: a "mito-window" on mitochondrial neurodegeneration. *Mol Cell Neurosci.* **55**, 62-76 (2013).
27. Su, B. *et al.* Abnormal mitochondrial dynamics and neurodegenerative diseases. *Biochim Biophys Acta.* **1802** (1), 135-142 (2010).
28. Vincent, A. M. *et al.* Mitochondrial biogenesis and fission in axons in cell culture and animal models of diabetic neuropathy. *Acta Neuropathol.* **120** (4), 477-489 (2010).
29. Leinninger, G. M. *et al.* Mitochondria in DRG neurons undergo hyperglycemic mediated injury through Bim, Bax and the fission protein Drp1. *Neurobiol Dis.* **23**, 11-22 (2006).
30. Leinninger, G. M., Edwards, J. L., Lipshaw, M. J., & Feldman, E. L. Mechanisms of disease: mitochondria as new therapeutic targets in diabetic neuropathy. *Nat Clin Pract Neurol.* **2**, 620-628 (2006).
31. Edwards, J. L. *et al.* Diabetes regulates mitochondrial biogenesis and fission in mouse neurons. *Diabetologia.* **53** (1), 160-169 (2010).
32. Fernyhough, P., Roy Chowdhury, S. K., & Schmidt, R. E. Mitochondrial stress and the pathogenesis of diabetic neuropathy. *Expert Rev Endocrinol Metab.* **5** (1), 39-49 (2010).
33. Schmidt, R. E., Green, K. G., Snipes, L. L., & Feng, D. Neuritic dystrophy and neuronopathy in Akita (Ins2(Akita)) diabetic mouse sympathetic ganglia. *Exp Neurol.* **216** (1), 207-218 (2009).

 

34. Penna, G. *et al.* Human benign prostatic hyperplasia stromal cells as inducers and targets of chronic immuno-mediated inflammation. *J Immunol.* **182** (7), 4056-4064 (2009).
35. Lentz, S. I. *et al.* Mitochondrial DNA (mtDNA) Biogenesis: Visualization and Duel Incorporation of BrdU and EdU Into Newly Synthesized mtDNA In Vitro. *J Histochem Cytochem.* **58** (2), 207-218 (2010).
36. Glas, U., & Bahr, G. F. Quantitative study of mitochondria in rat liver. Dry mass, wet mass, volume, and concentration of solids. *J Cell Biol.* **29** (3), 507-523 (1966).
37. Bertoni-Freddari, C. *et al.* Morphological plasticity of synaptic mitochondria during aging. *Brain Research.* **628** (1-2), 193-200 (1993).
38. Kaasik, A., Safiulina, D., Zharkovsky, A., & Veksler, V. Regulation of mitochondrial matrix volume. *Am J Physiol.* **292** (1), C157-163 (2007).
39. Misgeld, T., Kerschensteiner, M., Bareyre, F. M., Burgess, R. W., & Lichtman, J. W. Imaging axonal transport of mitochondria in vivo. *Nat Meth.* **4** (7), 559-561 (2007).
40. Park, J. Y. *et al.* Mitochondrial swelling and microtubule depolymerization are associated with energy depletion in axon degeneration. *Neuroscience.* **238**, 258-269 (2013).
41. Court, F. A., & Coleman, M. P. Mitochondria as a central sensor for axonal degenerative stimuli. *Trends Neurosci.* **35** (6), 364-372 (2012).
42. Baloh, R. H. Mitochondrial dynamics and peripheral neuropathy. *Neuroscientist.* **14** (1), 12-18 (2008).
43. Chowdhury, S. K., Smith, D. R., & Fernyhough, P. The role of aberrant mitochondrial bioenergetics in diabetic neuropathy. *Neurobiol Dis.* **51**, 56-65 (2013).
44. Kennedy, W. R., Wendelschafer-Crabb, G., & Johnson, T. Quantitation of epidermal nerves in diabetic neuropathy. *Neurology.* **47**, 1042-1048 (1996).
45. Lauria, G. *et al.* EFNS guidelines on the use of skin biopsy in the diagnosis of peripheral neuropathy. *Eur J Neurol.* **12** (10), 747-758 (2005).
46. Lauria, G. *et al.* European Federation of Neurological Societies/Peripheral Nerve Society Guideline on the use of skin biopsy in the diagnosis of small fiber neuropathy. Report of a joint task force of the European Federation of Neurological Societies and the Peripheral Nerve Society. *Eur J Neurol.* **17** (7), 903-912, e944-909 (2010).
47. Umapathi, T., Tan, W. L., Tan, N. C. K., & Chan, Y. H. Determinants of epidermal nerve fiber density in normal individuals. *Muscle Nerve.* **33** (6), 742-746 (2006).
48. Lauria, G. *et al.* Epidermal innervation: changes with aging, topographic location, and in sensory neuropathy. *J Neurol Sci.* **164** (2), 172-178 (1999).
49. Lauria, G. *et al.* Intraepidermal nerve fiber density at the distal leg: a worldwide normative reference study. *J Peripher Nerv Syst.* **15** (3), 202-207 (2010).
50. Hamid, H. S. *et al.* Hyperglycemia- and neuropathy-induced changes in mitochondria within sensory nerves. *Ann Clin Transl Neurol.* **1** (10), 799-812 (2014).


 